Optimization of Transdermal Drug Delivery by Hydrogel-Enhanced Sonophoresis

BEE 4530: Computer-Aided Engineering

Nate Chapin, Michelle Hung, Wesley Larsen, Varsha Pramil

Table of Contents

Executive Summary 2

Introduction 3

- **Problem Statement** 4
- **Design Objectives** 4
- **Governing Equations** 4
- **Initial Conditions** 6
- **Design Schematic** 7

Results 8

- **Preliminary Results** 8
- **Model Validation** 9
- **Sensitivity Analysis** 10
- **Optimization** 11

Discussion 13

- **Conclusion** 13
- **Future Recommendation** 13

Appendix A. Mesh Convergence 14

- **Mesh Implantation** 14
- **Mesh Convergence** 14

Appendix B. Model Design 16

- **Boundary Conditions** 16
- **Other terms** 16
- **Terms for Ultrasound Wave** 17
- **Input Parameters** 18

Appendix C. References 19

Executive Summary

External-field mediated transdermal drug delivery is a new alternative to oral delivery and hypodermic injections. This method allows patients to receive treatments via a drug-infused patch applied to the skin and offers continuous release of drug for up to a week. It is also relatively inexpensive compared to regular treatments. In our design, ultrasound and an applied electric field are used to increase the rate of drug diffusion and propagation from the patch into and across the skin. Previous research has shown that the application of ultrasound results in higher rates of transdermal transport by increasing the permeability of the stratum corneum. This permeabilization can be so great that the patch or drug reservoir itself becomes the most significant barrier to the overall transdermal drug transport. An applied voltage has been shown to be capable of creating a driving force for transport that counteracts this effect.

In this project, we combined the effects of applied voltage and ultrasound in order to model the transdermal transport of insulin from a methyl-cellulose hydrogel through the skin. Because the typical drug-delivery patch is circular, we modeled the problem in a 2D-axisymmetric geometry. Next, we determined the effects of intensity and voltage on the average insulin concentration in the skin. To do this, we conducted a sensitivity analysis by varying the applied voltages and intensities on the hydrogel and calculating the corresponding average insulin concentration in the skin at a specific time point. Finally, by using an objective function, we maximized the flux of insulin through the skin while minimizing patient discomfort.

The iontophoretic and sonophoretic aspects of our model were validated individually through comparison with experimental data. We found that voltage and intensity from ultrasound combined provide the greatest increase in insulin transport through the skin. An intensity of 1 kW/m^2 in conjunction with an applied voltage of -2 V resulted in the optimum insulin flux through the skin while maintaining minimal patient discomfort. The optimal intensity was found to be at the lower end of the range of experimentally and clinically utilized values. This suggests that higher intensities may contribute unnecessary heating without significantly enhancing insulin transport through the skin. Based on our optimization results, it can be seen that transdermal delivery of insulin through the skin is efficient when coupled with ultrasound and applied voltage.

Our results show that with the application of sonophoresis and iontophoresis, insulin is effectively able to diffuse through the skin into the bloodstream. Our optimization also shows that this type of insulin delivery would cause minimal discomfort or skin damage. This suggests that transdermal delivery of insulin through the skin is a promising treatment for patients with diabetes.

Introduction

Diabetes is the 7th largest cause of death in the United States, leading to lower life expectancy, heart disease, and kidney failure [1]. Patients with diabetes experience high medical care costs due to the regular insulin injections required to control glucose levels. In the United States, almost 23.6 million people are currently diagnosed with diabetes [2]. There are two types of diabetes: Type I and Type II diabetes. In Type I diabetes, the patient's pancreas is unable to produce the insulin that is needed to break down glucose into energy. In Type II diabetes, the patient's pancreas either does not produce enough insulin or their body cells do not recognize the insulin that is produced. Diabetics who can not produce any or enough insulin must find another way to maintain healthy blood-insulin levels.

Currently, the most common ways to increase the level of insulin in the bloodstream are through insulin injection or use of an insulin pump. However, both of these methods require insertion of a needle or cannulas. These methods can be painful and cause scarring.

Transdermal drug delivery is an alternative to hypodermic injections and pumps. The first transdermal delivery system was applied to motion sickness and was approved in the United States in 1979 [3]. Transdermal delivery has many advantages over hypodermic injections including less pain, reduction of dangerous medical waste, avoidance of certain disease transmission pathways, and low cost. However, there a limited number of drugs that can be effectively delivered transdermally because of the extremely low permeability of the epidermis. In particular, drugs that have high molecular weight or are strongly hydrophobic are difficult to apply transdermally [3]. Insulin is one of these drugs, with a molecular weight of 5808 Da.

In this study, insulin is transdermally delivered through skin via a hydrogel patch. However, since the high molecular weight of insulin inhibits it from easily passing through the skin, other agents are required in addition to the patch to increase the rate of insulin transport across the skin.

One of these agents is ultrasound transmission. Ultrasound creates cavitation- the formation, oscillation and collapse of bubbles- which generates shock waves and liquid microjets directed at the stratum corneum. This breaks apart the lipid structure of the stratum corneum and increases skin permeability, allowing more insulin to enter through the skin. Despite this benefit, penetration of ultrasound energy directly through the skin can be painful and dangerous. An ultrasound coupling medium such as a methyl-cellulose hydrogel can be used to mitigate the harmful effects of ultrasound. Unfortunately, this coupling medium can impede the diffusion of insulin through the skin. Voltage can be applied along with ultrasound and a coupling medium to counteract this hindrance. Experimental results have shown that with

the addition of a voltage potential, the diffusivity of insulin through the skin increases more so than when ultrasound energy was applied alone [2].

Problem Statement

Using COMSOL, we modeled the diffusion of insulin into the skin from a methyl-cellulose hydrogel reservoir in response to the application of low-frequency ultrasound and a voltage to the surface of the skin.

Design Objectives

Based on our desire to maximize insulin flux while minimizing patient discomfort and skin tissue damage, we decided on three design objectives for our study, which are listed below.

1. Develop an accurate model of transdermal insulin delivery that combines the effects of applied voltage and ultrasound
2. Conduct sensitivity analysis to determine the relative effect of applied voltage and ultrasound on insulin diffusion rate
3. Optimize the flux of insulin while minimizing patient discomfort using an objective function

Governing Equations

The governing equations for our model are discussed in detail below. The various terms and equations used to relate these equations to one another are included in Appendix A.

<u>Mass Species Conservation with Nernst-Planck</u>
Diffusion of insulin is modeled by calculating the concentration throughout the hydrogel and skin over time. The Nernst-Planck equation [Equation 1] is used because the species of interest, insulin, is a charged molecule.

$$\frac{\partial c}{\partial t} + \nabla \circ (-D\nabla c - zu_m Fc\,\bar{\nabla}\,V) = 0 \qquad \text{[Equation 1]}$$

The $-D\nabla c$ term describes diffusion within the materials and the $zu_m Fc\,\bar{\nabla}\,V$ term describes the bulk flow effect caused by the applied voltage. Diffusivity is a function of both temperature and ultrasound frequency, as described by the equations in Appendix B.

<u>Poisson Voltage Equation</u>
The Poisson equation [Equation 2] is used to calculate the voltage throughout the material.

$$J = -(\sigma + \varepsilon_0 \varepsilon_r \omega)E \qquad \text{[Equation 2]}$$

The calculated voltage depends on the applied voltage boundary condition, the electrical conductivity, vacuum permittivity, and relative permittivity. The electrical conductivity varies with temperature. The empirically derived equation describing this dependence is given in Appendix B for each material.

Helmholtz Equation

The Helmholtz equation [Equation 3] characterizes the pressure waves caused by ultrasound.

$$\frac{\partial}{\partial r}\left[-\frac{r}{\rho_c}\left(\frac{\partial P}{\partial r}\right)\right] + r\frac{\partial}{\partial z}\left[-\frac{1}{\rho_c}\left(\frac{\partial P}{\partial z}\right)\right] - \left[\left(\frac{\omega}{c_c}\right)^2\right]\frac{rP}{\rho_c} = 0 \qquad \text{[Equation 3]}$$

As can be seen in Equation 3, the pressure profile depends on the angular frequency of the ultrasound, ω, the complex density, ρ_c, and complex speed of sound in the medium c_c.

Heat Transfer Equation:

The heat transfer equation [Equation 4] is used to describe heat transfer within the materials.

$$\rho c_p \frac{\delta T}{\delta t} = \nabla \circ (k\nabla T) + Q \qquad \text{[Equation 4]}$$

Q, the heat generation term, is a function of ultrasound intensity and pressure as well as applied voltage. The exact formula is given in Appendix B. Metabolic heat generation is negligible compared to heat generated by ultrasound and the applied voltage, and so has been ignored. The thermal conductivity of each of the materials is dependent on temperature, with the general relationship being higher conductivity at higher temperature. The precise equations describing the thermal conductivity of each material have been obtained empirically and are given in Appendix B.

Figure 1 below shows the relationships between the terms in our model.

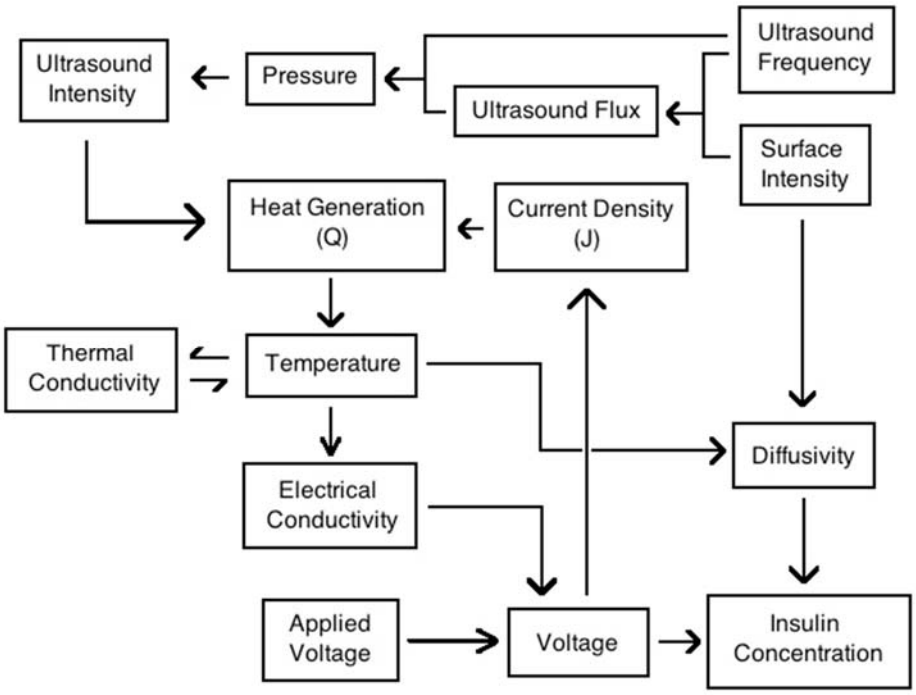

Figure 1. Interconnectivity of physics implemented in the model. Only three terms, ultrasound frequency, surface intensity and applied voltage are entirely independent. Terms such as temperature and voltage have many connections and are therefore expected to exhibit strong influence on the model as a whole.

As can be seen above, the terms associated with the Helmholtz equation are not dependent on the results of any of the other equations. The heat equation relies on terms calculated in the Helmholtz physics and the Poisson equation, which itself is dependent on the results of the heat equation. For this reason, the heat equation and Poisson equation are solved concurrently in our model. The Nernst-Planck equation requires variables calculated by the other equations but does not feed any values to them.

Initial Conditions

The initial concentration of insulin is 21.22 mol/m^3 in the hydrogel and zero in both the dermis and epidermis. This value was calculated such that the total amount of insulin in the patch meets an average patient's daily requirement and would be enough for several days [5]. The voltage and pressure are initially zero in all domains. Temperature in the hydrogel is set to room temperature, 298.15 K, and in the dermis and epidermis it begins at average body temperature, 310.15 K.

Design Schematic

For the purposes of the model, the skin is assumed to be semi-infinite in both the radial and axial directions. As shown below in Figure 2, our model is split into three distinct parts: the hydrogel, epidermis and dermis. Ultrasound and voltage are applied to the top surface of the circular patch, which has a radius of 2.5 cm and a thickness of 2.5 mm.

.

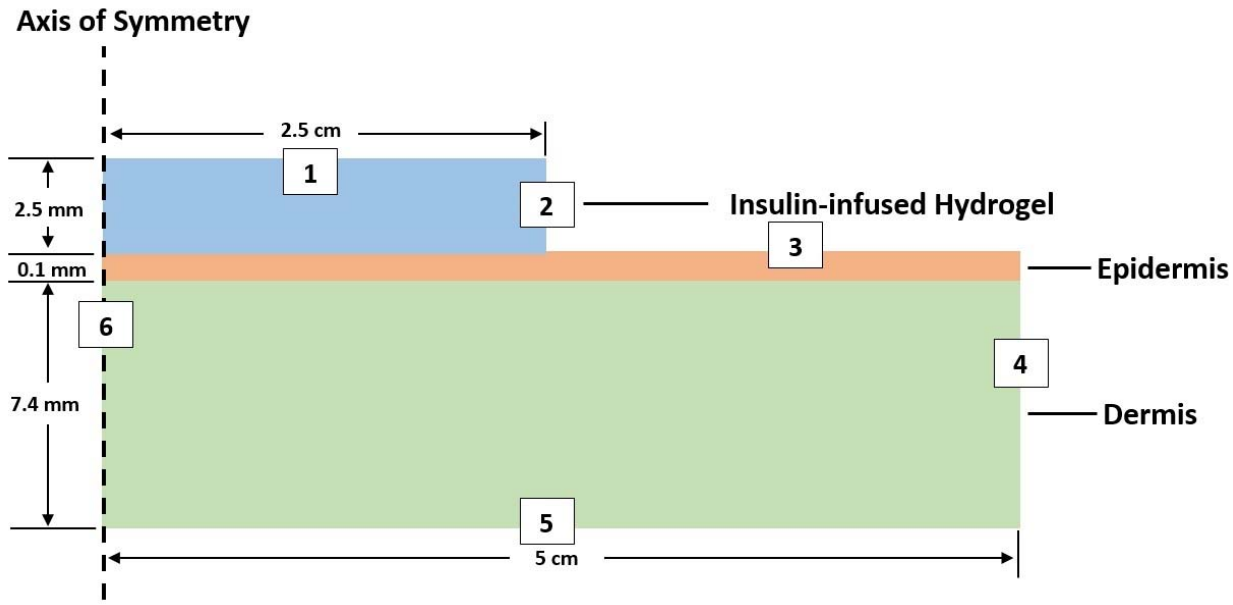

*Not to scale

Figure 2. Schematic of 2D axisymmetric geometry showing the insulin infused hydrogel, epidermis, and dermis layer with dimensions and boundary condition labels. The values for boundary conditions are shown in Table 2.

There are six boundaries in our model. Each boundary has a specific concentration, voltage, temperature, and ultrasound condition. These are all described below. Specific conditions corresponding to each boundary and physics can be found in Table 1 of Appendix B.

Concentration Boundary Conditions

At the skin and hydrogel surfaces (1, 2, and 3) there is assumed to be no loss of insulin by evaporation or other mechanisms, so a zero flux boundary condition is applied. Because the skin domain has been assumed semi-infinite, no insulin is expected to reach the far right boundary, 4, so concentration is set to zero there at all times. Similarly, the concentration of insulin at boundary 5 is assumed to remain zero as it is expected that all of the insulin that reaches that boundary will be carried away in the bloodstream. The axisymmetry of our model means that there is no flux of insulin across boundary 6.

Voltage Boundary Conditions

A constant A.C. voltage is applied to the top surface of the patch, so there is a constant voltage condition on boundary 1. The same semi-infinite and symmetry explanations apply to the voltage conditions on boundaries 4 and 5. At the skin surface and axis of symmetry (2, 3, and 6) there is no voltage flux.

Temperature Boundary Conditions

Boundaries 1, 2, and 3 are in contact with air, and so a convective boundary condition is applied to them. On boundary 4 and 5, the semi-infinite assumption means that temperature change never propagates to these boundaries, and they thus remain at body temperature. The axisymmetry of the model once again means that there is no flux across boundary 6.

Ultrasound Boundary Conditions

At the top of the hydrogel (1) there is a constant pressure flux caused by the applied ultrasound. There is no pressure flux at boundaries 2 and 3, as the pressure wave is assumed to be perpendicular or at boundary 4 due to the semi-infinite assumption, or at boundary 6 because of axial symmetry. At boundary 5 there is a no pressure flux condition in combination with an absorption condition which limits inward wave propagation as well as reflection at the boundary from inside. This ensures a physical solution.

Results

Preliminary Results

The figure below (Figure 3) shows the diffusion of insulin when there is no applied voltage or ultrasound. After an hour, the diffusion profile has only progressed to the epidermis.

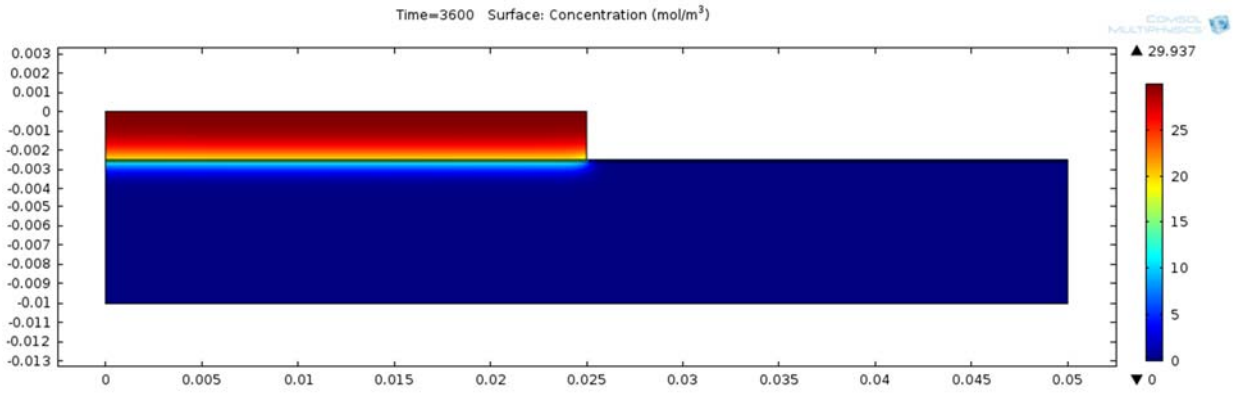

0 V, 0 I, 1 hr

Figure 3. Zero Voltage Concentration Plot Showing the Concentration Gradient Through Dermis and Epidermis

Because the diffusivity in the epidermis is 2-3 orders of magnitude lower than in the other regions, it serves as an obstacle to drug diffusion. This is why the concentration gradient is largest in the epidermis and near negligible in the other regions, demonstrating the need for both ultrasound and voltage applied across the surface.

Model Validation

Paired iontophoretic and sonophoretic transdermal drug delivery studies do not exist. For this reason, it was necessary to validate these aspects of our model individually. To validate the sonophoretic aspect of our model, our model was changed to match the specification of an experiment Ultrasound Mediated Transdermal Drug Delivery [27]. This study involved studying the transdermal insuling flux of insulin across a rat's epidermal membrane using a ultrasound applying transducer above a Franz diffusion cell. Conceptually, a Franz diffusion cell is essentially a beaker with a membrane stretched taut across the top with a reservoir of solution above the membrane. Solution that has diffused through can be tested in the beaker to determine the amount that has diffused through. Changes implemented include: making the geometry the same rectangular shape as the cell-epidermis system and changing the lower constant temperature boundary to convective heat flux.

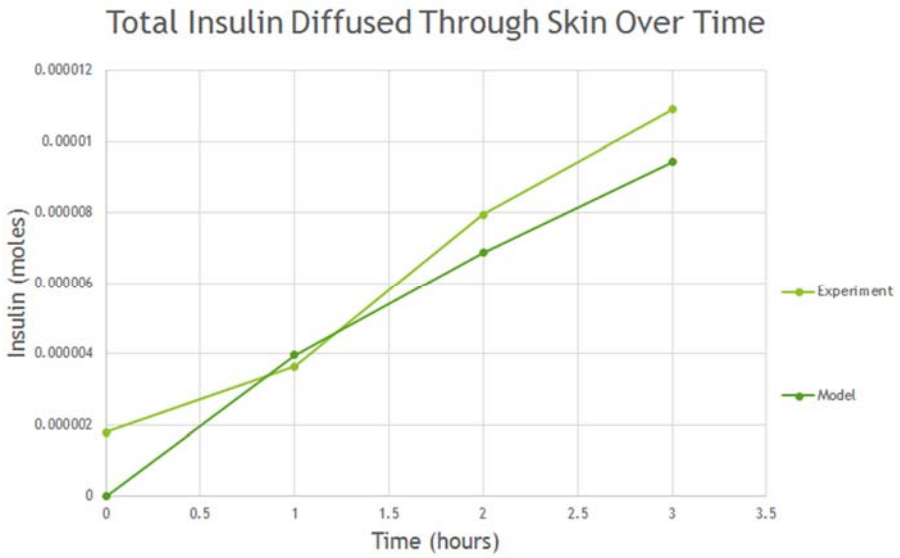

Figure 5. Ultrasound Mediated Transdermal Drug Delivery Validation

Calculating the total Insulin that has diffused through suggests that our model is validated by the study as the results are very similar. This shows that our implementation of ultrasound was successful in being a good model of the physics at hand.

To validate iontophoresis, the model was compared to a study entitled Transdermal Iontophoresis of Insulin IV: Effect of Chemical Enhancers Validation [26]. The protocol for the

study was exactly the same as the previous case: measuring drug permeated across an epidermal membrane in a Franz diffusion cell except that an anode and cathode were present to develop a Voltage across the membrane instead of the ultrasound transducer.

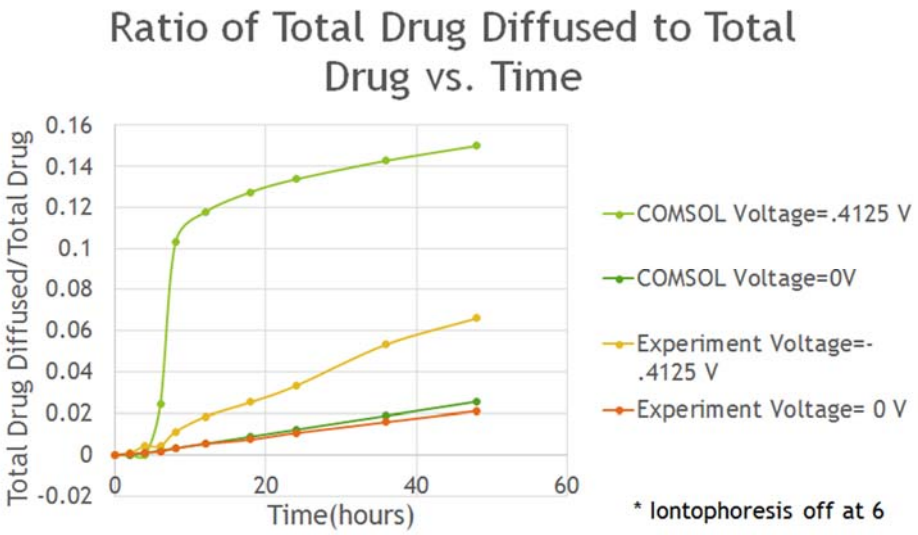

Figure 6. Transdermal Iontophoresis of Insulin IV: Effect of Chemical Enhancers

Validation

Our study of the passive impact without voltage was very successful and results are near identical. The results for voltage applied were not so successful. Although they are within the same order of magnitude and the actual difference between them is not great, the voltage results vary because the study used did not state a voltage applied, rather a current density applied. Thus to find voltage applied, Ohm's law was used which is not entirely accurate for skin due to non-linearities, and values for resistance were highly variable in the literature ranging from 100 ohms to 100 megaohms. Voltage applied could be arbitrarily changed to match our results to the results of the study, but this would not be useful in validation as the validation step is important in checking and confirming your results, not a way to reverse-engineer parameters.

Sensitivity Analysis

In order to determine the necessity of obtaining accurate values for certain parameters, a sensitivity analysis was conducted. Beginning with experimental measurements of specific heats and thermal conductivities of hydrogel and the epidermis, we increased and decreased the values by 10% . We then calculated the average concentration in the skin based on these property values, and the bar graph (Figure 9) shows the effects of these parameters on the solution.

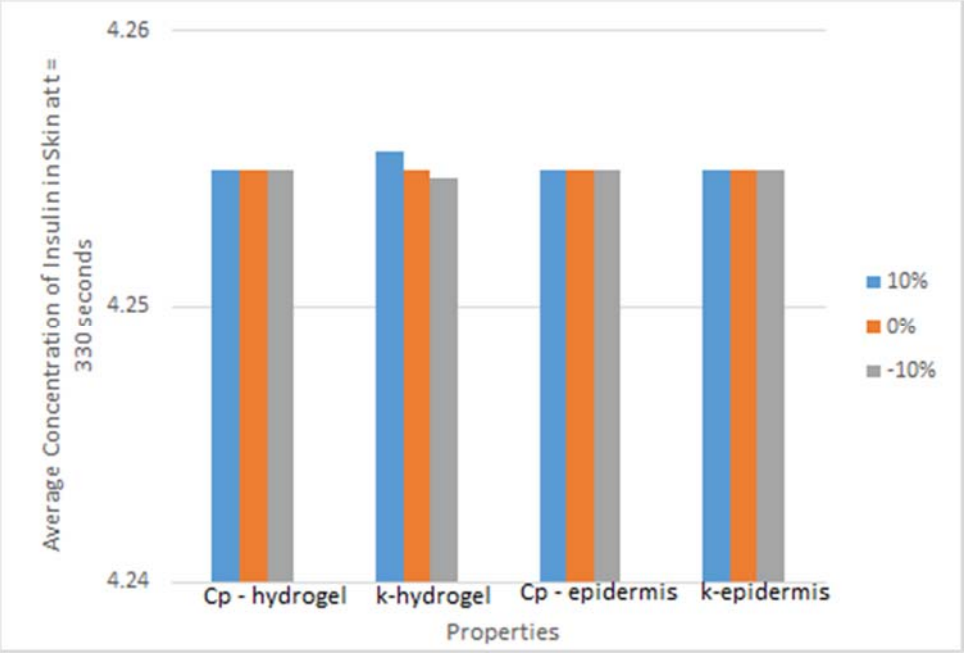

Figure 9. Variation in average concentration of insulin in skin at t = 330 minutes when the properties of hydrogel and epidermis are varied within ± 10% of their original value.

According to the above graph, the effects of varying the specific heats and thermal conductivities of the hydrogel and the epidermis show no significant effect on the average concentration of insulin in the skin. Based on this, we can assume that even if the experimental values we obtained for these parameters are not exact, this error would not significantly affect our solution.

In order to garner a fuller understanding of the effects of Iontophoresis and sonophoresis on transdermal drug transport we sought to run a sensitivity analysis on voltage and ultrasound. We were specifically interested in determining if the improvement in drug transport evidenced by the combination of these methods was predominantly due to one effect or the other.

In addition, an analysis of solution sensitivity to changes in applied voltage will allow us to check the accuracy of our model. The greater the applied voltage, the faster should be the rate of insulin transport, and the further the depth of its penetration at steady-state.

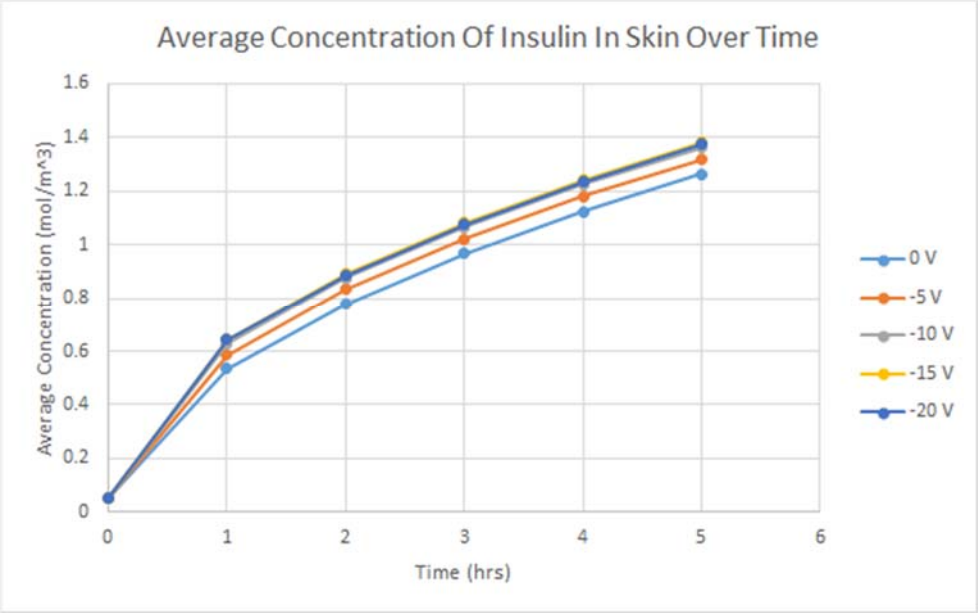

Figure 7. Average insulin concentration in the epidermis and dermis over for a range of voltages over time. It can be seen that the result is more heavily influenced by voltage changes at smaller voltages.

The fact that average concentration of insulin in the skin at a certain time point increases with increasing voltage shows that our model is consistent with previous research which has stated that increasing voltage can drive a charged molecule more quickly and thus that higher voltage will lead to faster transport.

Below (Figure 8), we show the dependence of the average insulin concentration in the skin on the intensity of ultrasound. Specifically, for insulin, enhanced subcutaneous delivery has been demonstrated with ultrasound over an intensity range of 0 - 8 kW/m^2. Therefore, we conducted our sensitivity analysis for these range of values.

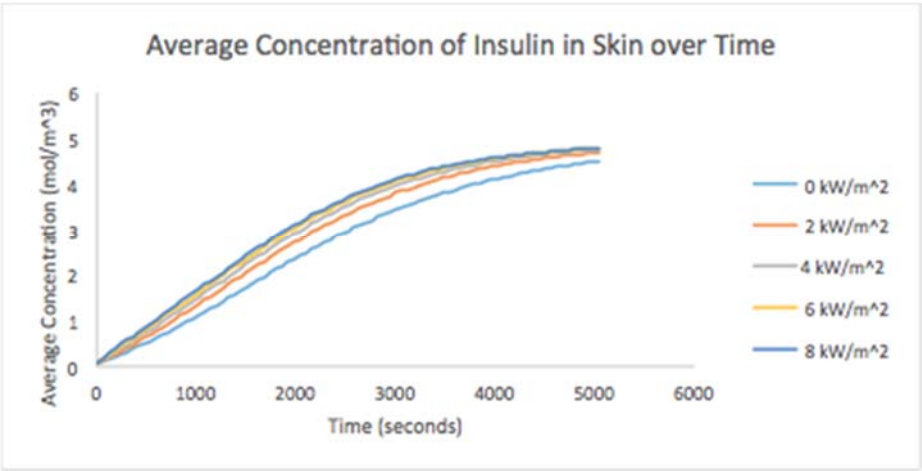

Figure 8. Average insulin concentration at the skin over for a range of surface intensities over time. It can be seen that at higher surface intensities, insulin passes through the skin more quickly.

Figure 8 shows that as the intensity of ultrasound increases, the concentration of insulin transported from the hydrogel into the skin increases.

Since both plots above show a dependence of the rate of insulin transport on the variable in question (voltage or intensity), it is clear that the optimal result will not be reached by considering either alone.

Optimization

I. Overview

Because our aim was to increase drug flux without causing the patient undue discomfort, the objective function we used to evaluate the effectiveness of each parameter set is described qualitatively as follows: The objective function value increases with greater flux at hydrogel-epidermis boundary (average over study time). It decreases with increasing CEM43 within an acceptable range, becoming zero if it exceeds the acceptable threshold. Finally, the function value decreases proportionally to some yet to be determined measure of pain due to voltage.

The function was optimized by maximizing its value over a range of applied AC voltages and ultrasound intensities.

II. Flux Term

The motivation for introducing ultrasound to transdermal drug-delivery processes is to increase drug delivery rate. When used in conjunction with a coupling medium, however, insulin diffusion through the hydrogel becomes the limiting factor, rather than diffusion into and across the stratum corneum (outermost layer of the epidermis). To combat this, an AC voltage is applied to facilitate diffusion through the hydrogel. Therefore, the overall goal is to increase the rate of drug delivery, with the primary concern being not diffusion through the stratum corneum and epidermis, as in traditional delivery methods, but out of the hydrogel. For this reason, flux at the hydrogel-epidermis boundary (F_{HE}) will be used as a measure of the success of a given setup.

III. Temperature Term

In order to quantify the effects of temperature rise, we will use CEM43, or cumulative equivalent minutes at 43 C. Though typically used as a measure of cell death, with a lower threshold it can be applied to our problem to describe skin damage and discomfort. The MRI +

EUREKA research consortium organized a workshop for discussion of thermal dose threshold models. One of the conclusions was that "9 CEM43 seems an acceptable thermal dose threshold for most patients." [16]. For this reason, the threshold we will use is 9 CEM43.

CEM43 = $\int_0^t tR^{(43-T)}dt$

R at T<43 = 0.25; R at T>43 = 0.5

T = average temperature during time period

IV. Objective Function and Results

The equation for the objective function, shown below, gives the objective function value as a difference between a scaled measurement of the average flux of insulin over the first hour and the CEM43 over that hour.

O.F.V. = 10^6*Average Flux - CEM43

The table below shows the objective function value for each set of parameters over which the model was optimized. Red X's represent parameters that cause excessive heating (CEM43 > 9).

	-1 V	-2 V	-3 V	-4 V	-5 V	-6 V	-7 V	-8 V
1 kW/m^2	16.82	**20.35**	20.20	18.90	X	X	X	X
2 kW/m^2	16.79	18.91	16.42	X	X	X	X	X
3 kW/m^2	10.92	X	X	X	X	X	X	X
4 kW/m^2	X	X	X	X	X	X	X	X
5 kW/m^2	X	X	X	X	X	X	X	X
6 kW/m^2	X	X	X	X	X	X	X	X
7	X	X	X	X	X	X	X	X

kW/m^2								
8 kW/m^2	X	X	X	X	X	X	X	X

Table 1. Optimization parameters and results of objective function. The prevalence of X's signifies that many experimentally used sets of parameters would be unlikely to be popular in clinical treatments as they are likely to cause patient discomfort.

The optimum parameters, as apparent above, are an applied voltage of -2 V and an ultrasound intensity of $1kW/m^2$. These parameters give an average insulin flux of $2.05*10^{-5}$ mol/m^2s, which corresponds to $1.45*10^{-4}$ moles of insulin transported across the epidermis in the one hour period. As can be seen above, there are only eight sets of parameters that do not overheat the model. This is more reasonable than it may seem because the challenge in transdermal drug delivery is not overcoming the diffusion barriers, but overcoming them in a way that is amenable to patients.

Discussion

Conclusion

Based on our optimization results, we can conclude that an applied voltage of - 2 V and an ultrasound intensity of $1kW/m^2$ are ideal for transdermal delivery of insulin. These parameter values are at the lower end of the range that have been tested in previous research. This shows that a higher ultrasound intensity or applied voltage can cause unnecessary heating to the patient's skin, leading to increased skin damage and discomfort without significantly increasing the flux of insulin.

Future Recommendations

This model could be easily adapted to apply to other drug molecules for which transdermal delivery is being considered. In addition, the use of alternate coupling media might allow the ultrasound intensity to be increased further without causing pain to the patient. Future study into the application of short-duration, higher intensity pulses of voltage and ultrasound might also produce interesting results.

Appendix A. Mesh Convergence

Mesh Implantation

Mesh convergence was done for diffusion, where rectangular mesh was applied with a mapped distribution. The number of elements in the distribution is 50 and the boundary selected was the axis of symmetry. In figure 2 mapped distribution is shown in different layers of the model, with the epidermis having the most dense distribution.

In the Helmholtz portion, a free triangular mesh was used with the maximum element size $\frac{1550(m/s)}{f}$. As shown in figure 3, the free triangular mesh is most concentrated at the epidermis and the top of dermis layer.

We varied the values for maximum element size (max_e), minimum element size (min_e), maximum element growth rate (growR), resolution of curvature (ResCurv), and resolution of narrow regions (ResNar). We decided to use the preset "Extremely fine" mesh, for which the values are 0.001 for max_e, 2e-6 for min_e, 1.1 for growR, 0.2 for ResCurv and 1 for ResNar.

Figure 2. Plot with rectangular mesh for Nernst-Planck, Heating, and Voltage.

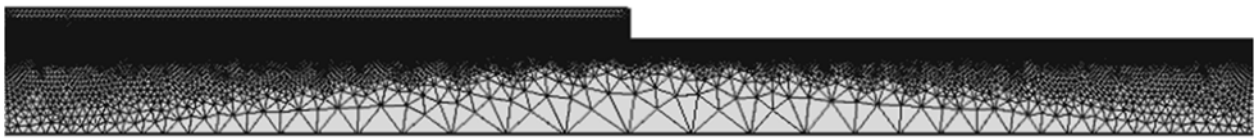

Figure 3. Plot with triangular mesh for Ultrasound.

Mesh Convergence

Mesh convergence was performed through a parametric sweep for the diffusion model, where we input the number of elements to be a global parameter and named it "element". After inputting the values for "element," we created a parametric sweep which ran through the elements of 1, 4, 8, 12, 25, 50, and 100. When the computing process was complete, we plotted a point graph, resulting in the plot shown in figure 14. As the parameter "element" increases, the change between successive concentrations profiles decreases.

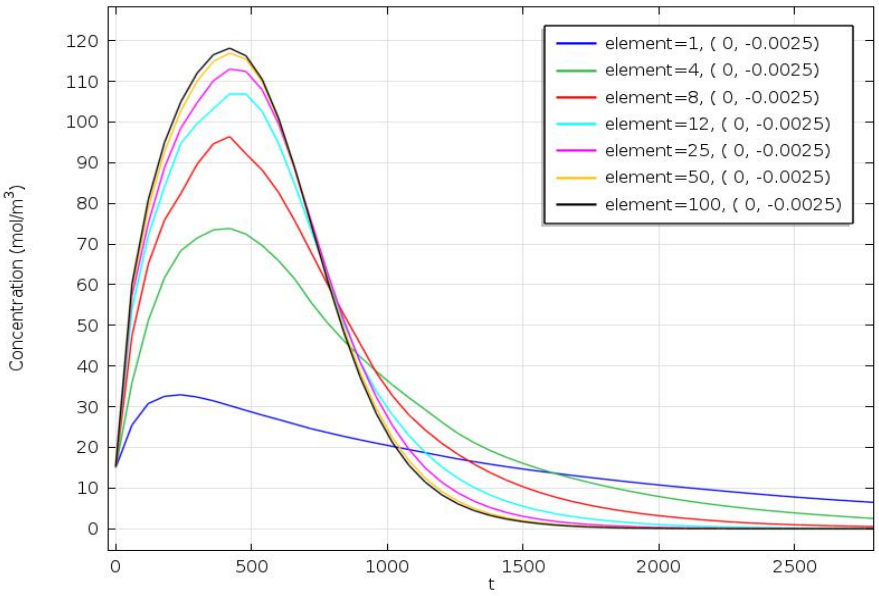

Figure 14. Mesh convergence for concentration at different times as shown with different numbers of elements.

By plotting the average concentration of the insulin in the skin over a variety of mesh sizes we were able to determine the approximate fineness of mesh that is needed. As the number of elements increased, the average concentration of insulin converges to a value. The mesh convergence was done at 3600s, where the curve converges at approximately 8000 elements as shown in figure 15. This showed the minimum mesh required in our model is about 8000 elements, and by using a mesh with 8000 elements or more we are not introducing significant discretization error to our model. We refrain from using a mesh much finer than 8000 elements in order to reduce the computing time of our model.

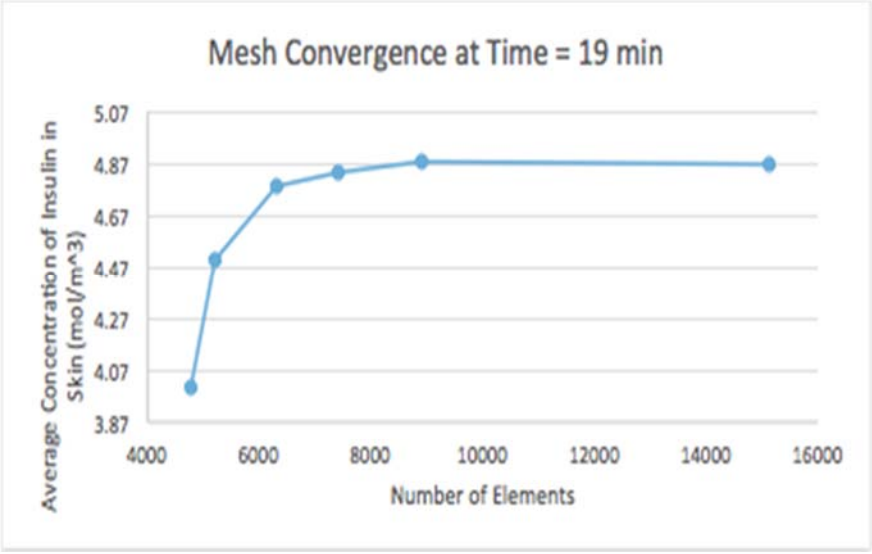

Figure 15. Mesh convergence for concentration at time = 3600 s with varied number of elements.

Appendix B. Model Design

Boundary Conditions

Boundary	Nernst-Planck	Poisson	Heat Equation	Helmholtz
1	$Flux_c = 0$	$V = V_S$	$Flux_T = h(T-T_{inf})$	$Flux_P = -2\pi f(I/\rho/c)^{1/2}$ Boundary absorption=0
2	$Flux_c = 0$	$Flux_V = 0$	$Flux_T = h(T-T_{inf})$	$Flux_P = 0$
3	$Flux_c = 0$	$Flux_V = 0$	$Flux_T = h(T-T_{inf})$	$Flux_P = 0$
4	$Flux_c = 0$	$V = 0$	$T = T_{body}$	$Flux_P = 0$
5	$c = 0$	$V = 0$	$T = T_{body}$	$Flux_P = 0$, Boundary absorption=i*k/rho_c
6	$c = 0$	$Flux_V = 0$	$Flux_T = 0$	$Flux_P = 0$

Other Terms

Name	Equation
Acoustic Heat Source	$Q = 2\alpha_{ABS}I + \nabla J$
Temperature Dependence of Human Tissue Thermal Conductivity	$k = 0.4692 + 0.0012*(T-273.15)$
Temperature Dependence of Hydrogel Thermal Conductivity	$k = k_{298.15}*(1+0.0015*(T-298.15))$
Skin Diffusivity Temperature Dependence	$D = D_{310.15}*(1 + 0.152778*(T-310.15))$
Hydrogel Diffusivity Temperature Dependence	$D = D_{298.15}(1 + 0.015*(T-298.15))$
Tissue (liver) Electrical Conductivity Temperature Dependence	$\sigma = 0.0078*T - 1.9827$
Hydrogel Electrical Conductivity Temperature Dependence	$\sigma = 1.3*(1.02)^{abs(T-298.15)}$
Effective Diffusivity for Epidermis	$D_{eff} = K_p^{us}(L_{gel}+h)$
Permeability Coefficient in the Presence of Ultrasound	$K_p^{us}=194K_m(fD^{\infty}+(1-f)D_0)$
Permeant Diffusion Coefficient	$D_0=K_P^P/(194K_m)$

Partition Coefficient	$K_m=K_{O\|W}^{.75}$
Fraction of area of unordered lipid bilayer	$f=.15663/(R/R_0)-.14269$
Linear Regression of Resistance Reduction against Ultrasound Duty and Intensity (Duty is 1 in our model)	$R/R_0=.84318-.08411(Intensity)$

[11] [12] [13] [17] [18] [19] [21]

Terms for Ultrasound Wave

Intensity of the ultrasonic wave	$I = \sqrt{I_z^2 + I_\varphi^2 + I_r^2}$
Wave intensity in the axial direction	$I_z = 0.5 * (p \cdot v_z)$
Wave intensity in the angular direction	$I_\varphi = 0.5 * (p \cdot v_\varphi)$
Wave intensity in the radial direction	$I_r = 0.5 * (p \cdot v_r)$
Velocity in axial direction	$v_z = -\frac{\frac{dp}{dz}}{(\rho_c * i * \omega)}$
Velocity in angular direction	$v_\varphi = -\frac{\frac{dp}{d\varphi}}{(\rho_c * i * \omega)}$
Velocity in radial direction	$v_r = -\frac{\frac{dp}{dr}}{(\rho_c * i * \omega)}$
Complex density	$\rho_c = \rho_t * \left(\frac{c_0}{c_c}\right)^2$
Complex speed of sound	$c_c = \frac{\omega}{k}$
Wave moves in k direction	$k = \left(\frac{\omega}{c_0}\right) - (i * \alpha)$

[25]

Input Parameters

Epidermal Thermal Conductivity ($\mathbf{k_{epidermal}}$)	0.59 W/mK
Dermal Thermal Conductivity ($\mathbf{k_{dermal}}$)	0.4 W/mK
Hydrogel Thermal Conductivity	0.6096 W/mK
Epidermal Density ($\boldsymbol{\rho_{epidermal}}$)	1044 kg/m^3
Dermal Density ($\boldsymbol{\rho_{dermal}}$)	1048 kg/m^3
Hydrogel Density ($\boldsymbol{\rho_{hydrogel}}$)	999.997 kg/m^3
Epidermal Specific Heat ($\mathbf{C_{p,epidermal}}$)	3710 J/kgK
Dermal Specific Heat ($\mathbf{C_{p,dermal}}$)	3650 J/kgK
Diffusivity, dermis ($\mathbf{D_{dermis}}$)	5.8e-11 m^2/s
Diffusivity, epidermis ($\mathbf{D_{epidermis}}$)	1.58e-13 m^2/s
Diffusivity, hydrogel ($\mathbf{D_{hydrogel}}$)	1e-10 m^2/s
Diffusivity, voltage ($\mathbf{D_{voltage}}$)	3.6e-3 m^2/s
Alpha, hydrogel	0.0251 /m
Alpha, skin	8.55 /m
Hydrogel Electrical Conductivity	1.3 S/m
Dermis Electrical Conductivity	0.44 S/m
Epidermis Electrical Conductivity	0.44 S/m
Permeant Diffusion Coefficent in a Disordered Bilayer (D^{∞})	1.17422 e-6 cm^2/sec
Octanal/Water Partition Coefficient of Insulin ($K_{O\|W}$)	.017378
Passive Permeability Coefficient (K_P^P)	3.25 e-8 cm/sec
Thickness of Gel (L_{gel})	.0025 m
Thickness of Epidermis (h)	.000015 m

Table 3. List of input parameters for our model. Values are given at 310.15 K for skin parameters and 298.15 K for hydrogel parameters. [18] [20]

Appendix C. References

[1] O. M. Hassan, et al., "Modeling of ultrasound hyperthermia treatment of breast tumors," in Radio Science Conference, 2009. NRSC 2009. National, 2009, pp. 1- 8.

[2] Zhang, Ingrid, K. Kirk Shung, and David A. Edwards. "Hydrogels with Enhanced Mass Transfer for Transdermal Drug Delivery." *Journal of Pharmaceutical Sciences* 85.12 (1996): 1312-316. Web. 10 Feb. 2015.

[3] Prausnitz, Mark R., and Robert Langer. "Transdermal Drug Delivery." *Nature biotechnology* 26.11 (2008): 1261–1268. *PMC*. Web. 12 Feb. 2015.

[4] COMSOL. (2013, February 12, 2014). Focused ultrasound induced heading in tissue phantom. Available: http://www.comsol.com/model/focused-ultrasound-induced-heating-in-tissue-phantom-12659

[5] "Patch That Could Replace Insulin Jabs for Diabetics." *Mail Online*. Accessed February 27, 2015. http://www.dailymail.co.uk/health/article-2184599/Patch-replace-insulin-jabs-diabetics.html.

[6] "The U-Strip – Insulin Patch | PDF." *Transdermal Specialties*. Web. 27 Feb. 2015. <http://www.transdermalspecialties.com/u-strip-patch.html>.

[7] Bloomgarden, Zachary T. "Aspects of Insulin Treatment." *Diabetes Care* 33, no. 1 (January 1, 2010): e1–6. doi:10.2337/dc10-zb01.

[8] "Diabetes | Insulin Therapy." *Diabetes*. Web. 27 Feb. 2015. <http://familydoctor.org/familydoctor/en/diseases-conditions/diabetes/treatment/insulin-therapy.html>.

[9] "Insulin Patch - How The Insulin Patch Works, Challenges, Research." Accessed February 27, 2015. http://www.diabetes.co.uk/insulin/insulin-patch.html.

[10] Mitragotri, S., D. A. Edwards, D. Blankschtein, and R. Langer. "A Mechanistic Study of Ultrasonically-Enhanced Transdermal Drug Delivery." *Journal of Pharmaceutical Sciences* 84, no. 6 (June 1995): 697–706.

[11] Tang, Hua, Daniel Blankschtein, and Robert Langer. "Effects of Low-Frequency Ultrasound on the Transdermal Permeation of Mannitol: Comparative Studies with in Vivo and in Vitro Skin." *Journal of Pharmaceutical Sciences* 91, no. 8 (August 2002): 1776–94. doi:10.1002/jps.10164.

[12] Cancel, Limary M., John M. Tarbell, and Abdellaziz Ben-Jebria. "Fluorescein Permeability and Electrical Resistance of Human Skin during Low Frequency Ultrasound Application." *The Journal of Pharmacy and Pharmacology* 56, no. 9 (September 2004): 1109–18. doi:10.1211/0022357044193.

[13] Tominaga, Kenji, and Kakuji Tojo. “Effect of Environmental Temperature on Transdermal Drug Penetration.” *Biological & Pharmaceutical Bulletin* 33, no. 12 (2010): 1983–87.

[14] Lee, Seungjun, Benjamin Snyder, Robert E. Newnham, and Nadine Barrie Smith. "Noninvasive Ultrasonic Transdermal Insulin Delivery in Rabbits Using the Light-Weight Cymbal Array." Diabetes Technology & Therapeutics 6.6 (2004): 808-15. Web.

[15] "Mechanisms of Action - Focused Ultrasound Foundation." Accelerating the Development and Adoption of Focused Ultrasound. Focused Ultrasound Foundation, n.d. Web. 23 Mar. 2015.

[16] Rhoon GC, Samaras T, Yarmolenko PS, Dewhirst MW, Neufeld E, Kuster N. 2013. CEM^{o}C thermal dose thresholds: a potential guide for magnetic resonance radiofrequency exposure levels? *Eur Radiol*. 23(8):2215-2227.

[17] Bhattacharya, A., and R. L. Mahajan. “Temperature Dependence of Thermal Conductivity of Biological Tissues.” *Physiological Measurement* 24, no. 3 (August 2003): 769–83.

[18] Ramires, Maria L. V., Carlos A. Nieto de Castro, Yuchi Nagasaka, Akira Nagashima, Marc J. Assael, and William A. Wakeham. “Standard Reference Data for the Thermal Conductivity of Water.” *Journal of Physical and Chemical Reference Data* 24, no. 3 (May 1, 1995): 1377–81. doi:10.1063/1.555963.

[19]Wood, D. G., M. B. Brown, and S. A. Jones. “Understanding Heat Facilitated Drug Transport across Human Epidermis.” *European Journal of Pharmaceutics and Biopharmaceutics* 81, no. 3 (August 2012): 642–49. doi:10.1016/j.ejpb.2012.03.019.

[20] Rao, C. N. R., and Ajay K. Sood. *Graphene: Synthesis, Properties, and Phenomena*. John Wiley & Sons, 2013.

[21] Mani, Anand. "Critical Evaluation of Current Skin Thermal Property Measurements." 8 May 2013. Web. 27 Apr. 2015. <http://www3.nd.edu/~msen/Teaching/UnderRes/SkinProperties.pdf>.

[22] Zurbuchen, Urte, Christoph Holmer, Kai S. Lehmann, Thomas Stein, André Roggan, Claudia Seifarth, Heinz-J. Buhr, and Jörg-Peter Ritz. “Determination of the Temperature-Dependent Electric Conductivity of Liver Tissue Ex Vivo and in Vivo: Importance for Therapy Planning for the Radiofrequency Ablation of Liver Tumours.” *International Journal of Hyperthermia: The Official Journal of European Society for Hyperthermic Oncology, North American Hyperthermia Group* 26, no. 1 (February 2010): 26–33. doi:10.3109/02656730903436442.

[23] Peyrot, Mark, Richard R. Rubin, Davida F. Kruger, and Luther B. Travis. “Correlates of Insulin Injection Omission.” *Diabetes Care* 33, no. 2 (February 2010): 240–45. doi:10.2337/dc09-1348.

[24] Smith, Nadine Barrie. “Perspectives on Transdermal Ultrasound Mediated Drug Delivery.” *International Journal of Nanomedicine* 2, no. 4 (December 2007): 585–94.

[25] Carter, Matt, Art Sullivan, Kenny Byers, and Michael Jessel. "Optimizing Ultrasonic

Intensity for High Intensity Focused Ultrasound Therapy." Computer Aided Engineering: Application to Biomedical Process. Web. 7 May 2015.
[26] Pillai, Omathanu, Vinod Nair, and Ramesh Panchagnula. "Transdermal iontophoresis of insulin: IV. Influence of chemical enhancers." *International journal of pharmaceutics* 269.1 (2004): 109-120.
[27] Kost, Joseph, and Robert Langer. "Ultrasound-mediated transdermal drug delivery." *Topical Drug Bioavailability, Bioequivalence, and Penetration*. Springer US, 1993. 91-104.